

Effect of annealing and initial temperature on mechanical response of a Ni–Ti–Cr shape-memory alloy

Jeom Yong Choi¹, Sia Nemat-Nasser*

*Center of Excellence for Advanced Materials, Department of Mechanical and Aerospace Engineering,
University of California, San Diego, 9500 Gilman Drive, La Jolla, CA 92093-0416, USA*

Received 11 February 2005; received in revised form 19 May 2006; accepted 19 May 2006

Abstract

The effect of the annealing conditions and the initial temperature on the compressive response of a ternary Ni–Ti–Cr shape-memory alloy is investigated at a strain rate of 10^{-3} /s, using an Instron hydraulic testing machine. The annealing temperature and duration considerably influence the forward, from austenite to the stress-induced martensite, and the reverse phase transformation. The transition stress and the yield stress of the resulting stress-induced martensite increase with the increasing annealing temperature. The transition stress reaches its maximum value for an annealing temperature of 573 K, and the yield stress for 673 K. Thereafter, both stresses decrease with further increase in the annealing temperature. The highest transition stress is attained for the smallest precipitates. In addition, the phase transformation upon cooling and heating changes from a single-step to a multiple-step with the decreasing annealing temperature. The transition stress for the stress-induced martensite formation increases with increasing initial temperature at a rate of about 8.5 MPa/K. The optimum annealing condition that produces the highest transition and yield stresses without an accompanying residual strain is 573 K for 60 min.

© 2006 Elsevier B.V. All rights reserved.

Keywords: Initial temperature; Transition stress; Yield stress; Clausius-Clapeyron slope; Superelastic property

1. Introduction

Shape-memory alloys have been extensively studied for various applications, particularly because of their superelastic property, i.e. a dissipative hysteretic response in loading and unloading without a permanent residual strain [1–5]. This superelastic property is due to a martensitic phase transformation, which can be induced by the application of an external stress at some temperature above M_s . Recently, it has been suggested that this superelastic property may be used for energy absorption (e.g. seismic protection of structures [5,6]).

The superelastic property of alloys can be improved by the suppression of the dislocation-induced slip deformation during the stress-induced martensite formation. This is attained by increasing the critical dislocation-induced slip stress [7–12]. In

particular, Huang and Liu [13] and Nemat-Nasser and Guo [14] have studied the effect of annealing temperature on the superelastic response of Ni–Ti shape-memory alloys. They point out that the transition stress for the stress-induced martensite formation decreases with the increasing annealing temperature. In particular, it is reported that the dissipated energy of the Ni–Ti shape-memory alloy, given by the area within the hysteresis loop, attains a minimum when the annealing temperature reaches about 600 K [14]. In addition, considerable effort has been focused on studying the effect of compositional changes on the mechanical and phase transformation properties of Ni–Ti–X ternary alloy systems [15–18]. It has been observed that the addition of Fe or Nb to Ni–Ti alloys improves their superelastic property by lowering the transformation temperature [17,19]. Recently, Cr has been found to be a promising candidate for tailoring the superelastic property of Ni–Ti alloys. Uchil et al. [20] have studied the transformation behavior of a Ni–Ti–Cr alloy in relation to its heat treatment conditions. They report that the phase transformation step of the alloy depends on the heat-treatment temperature: $A \leftrightarrow R$ at annealing temperatures below 673 K, $A \leftrightarrow R \leftrightarrow M$ at temperatures 673–873 K, and $A \leftrightarrow M$ at temperatures above 873 K. Here, A denotes the austenite phase

* Corresponding author. Tel.: +1 858 534 4914; fax: +1 858 534 2727.

E-mail addresses: jjeomyong@posco.co.kr (J.Y. Choi),
sia@ucsd.edu (S. Nemat-Nasser).

¹ Present address: POSCO, Technical Research Laboratories, 1 Goedong-dong, Nam-Gu, Pohang, Kyeongbuk 790-785, Republic of Korea.
Tel.: +82 54 220 6152.

with a CsCl structure, *R* denotes the phase with a rhombohedral structure, and *M* denotes the martensite phase with a monoclinic structure. We are not aware of any study that addresses the mechanical property of Ni–Ti–Cr shape-memory alloys at various initial temperatures and at various annealing conditions.

In the present study, we report some recent experimental results on the mechanical response, especially the superelastic property of a Ni–Ti–Cr alloy that is annealed at various temperatures and durations. After determining the optimum annealing condition, the superelastic response of the corresponding annealed Ni–Ti–Cr is investigated at a strain rate of 10^{-3} /s for a range of initial temperatures.

2. Experimental procedure

A hot-rolled 52.62 at.% Ni–47.09 at.% Ti–0.29 at.% Cr shape-memory alloy rod of 6.35 mm diameter is secured from Special Metals Corporation. Circular cylindrical samples of 5 mm nominal diameter and 5 mm nominal length are cut by electro-discharge machining (EDM). The specimens are annealed at temperatures between 473 and 1123 K for various durations in air, followed by water quench to a temperature of 292 K (see Table 1).

Quasi-static compression tests are performed at a strain rate of 10^{-3} /s and at various initial temperatures, to maximum strains within or exceeding the superelastic range, using an Instron hydraulic testing machine. A high-intensity quartz lamp is used to attain elevated temperatures. For low initial temperatures, a specially designed bath is used to control the temperature to within ± 2 K. The temperature is measured by a thermocouple, attached to the sample surface. The specimen deformation is measured by an LVDT, mounted in the testing machine and calibrated before each test. To reduce the end friction, the sample ends are lightly polished and greased prior to each test.

The transformation temperatures for the annealed alloy are determined using a differential scanning calorimeter (DSC Q10). Measurements are carried out at temperatures from 123 to 333 K under a controlled heating and cooling rate of 10 K/min. In addition, the specimen is held for 5 min at both the maximum and the minimum temperature.

The microstructure of some of the samples is examined by a Philips CM200, operated at 200 kV, using a side entry type double-tilt specimen holder. Samples for TEM observations are

cut with a low-speed diamond saw, parallel to the compression axis. Thin foils are prepared by grinding the cut sheets to about 150–100 μ m, and then they are thinned by twin-jet electro-polishing with an electrolyte of acetic acid and perchloric acid, 9:1 volume, at 296 K.

3. Experimental results and discussion

3.1. Annealing temperature effect

To investigate the overall mechanical properties of this Ni–Ti–Cr alloy, specimens are annealed at various temperatures for 10 min, and then quenched in water at 292 K. Fig. 1(a) and (b) shows the effect of annealing temperature on the stress–strain curve of the alloy, deformed at a strain rate of 10^{-3} /s and at 296 K initial temperature. In the case of the specimens that are deformed to strains exceeding approximately 0.1 (solid lines), the stress–strain curves show two transition stresses. These are

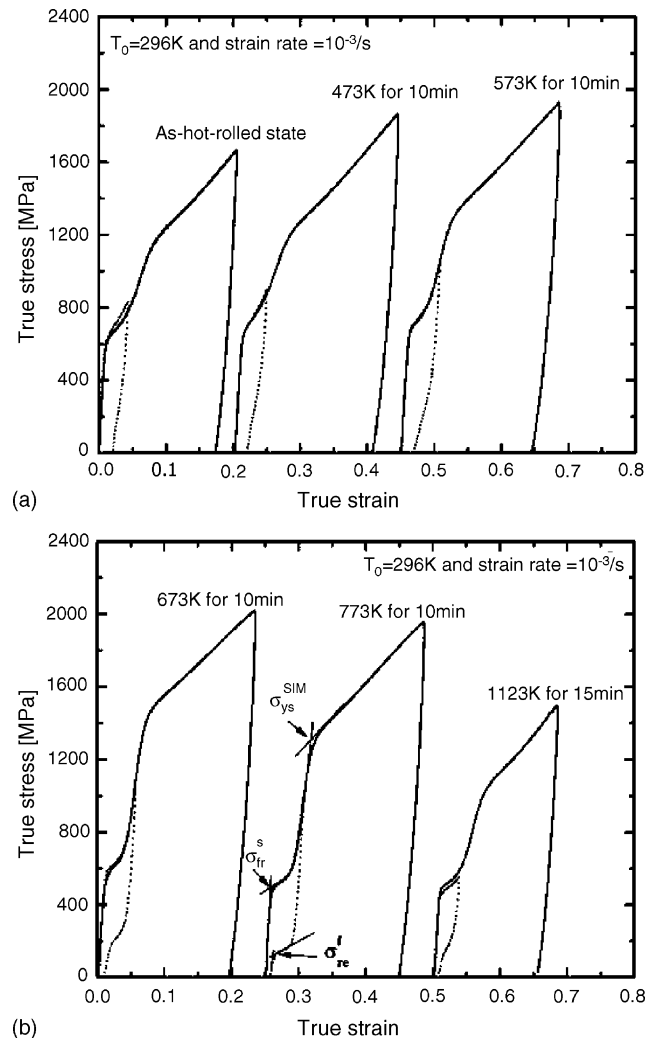


Fig. 1. Comparison of the stress–strain curves for a Ni–Ti–Cr alloy that is annealed under the indicated conditions and deformed within (dotted line) and beyond the superelastic regime (solid line) at 296 K initial temperature and at a 10^{-3} /s strain rate: (a) annealing temperature below 573 K and (b) annealing temperature above 573 K.

Table 1
Annealing treatment conditions

Temperature (K)	10 min	30 min	60 min	120 min	240 min
As-hot-rolled	–	–	–	–	–
473	✓	–	–	✓	✓
523	✓	–	–	–	–
543	–	✓	✓	–	–
573	✓	✓	✓	–	–
673	✓	✓	✓	–	–
773	✓	✓	✓	–	–
973	✓	✓	✓	–	–
1123 ^a	✓	–	–	–	–

^a 15 min.

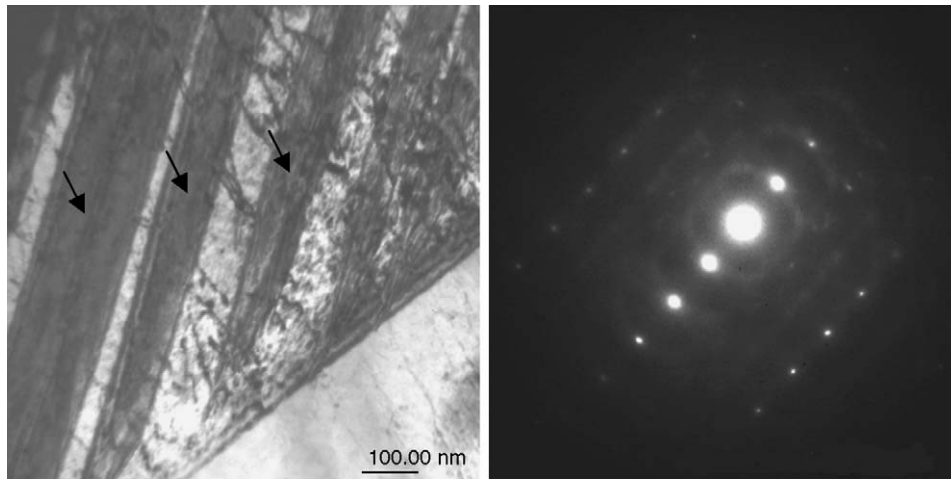


Fig. 2. TEM micrographs of a superelastically deformed Ni-Ti-Cr alloy that was annealed at 573 K for 10 min. The arrows indicate the residual stress-induced martensites.

defined by the intersection of the lines tangent to the ascending and the flat sections of the stress-strain curve. The lower transition stress corresponds to the forward transformation stress for the stress-induced martensite formation, σ_{fr}^s . The upper data correspond to the yield stress of the resulting martensite, σ_{ys}^{SIM} . These results are typical for shape-memory alloys that are deformed at a temperature in the range of M_s to M_d , where the response consists of an initial elastic deformation of the austenite, followed by the formation of the stress-induced martensite, and finally the elastic-plastic deformation of the resulting martensite. Here, M_s denotes the martensite transformation-start temperature on cooling, and M_d denotes the maximum temperature for the stress-induced martensite formation.

The superelastic response of the annealed specimens is also investigated at 296 K initial temperature. The samples are deformed to about 0.05 strain, estimated from the stress-strain curves, and then unloaded to zero stress. Here, the maximum strain is restricted to a certain level to ensure superelasticity, avoiding the dislocation-induced plastic slip. The resulting stress-strain curves (dotted lines) exhibit another lower transitional plateau regime, corresponding to the reverse transformation from the stress-induced martensite to the austenite. The finish stress for the reverse transformation from the stress-induced martensite to the austenite, σ_{re}^f , is also shown in Fig. 1. Even though annealed specimens are deformed within the (estimated) superelastic regime, the stress-strain curves show residual strains. These residual strains decrease with the increase in the annealing temperature. It is also observed that a plateau region appears in the reverse transformation on the unloading portion of the stress-strain curve, as the annealing temperature increases. For annealing temperatures below 573 K, the start and finish stresses for the reverse transformation are not clearly present, but they are clearly observed for annealing temperatures above 573 K.

Fig. 2 shows the TEM micrograph of the sample that has been annealed at 573 K for 10 min, and then deformed within the superelastic regime. Residual martensites (arrow) and extensive residual dislocations are clearly observed in this figure even

though the material has been deformed within the superelastic regime. This micrograph shows the presence of residual martensites that are left over through their interaction with the pre-existing dislocations. These residual martensites in the austenite matrix are stabilized by the residual dislocations [21] that had been produced in the hot-rolling process. Here, the defect structure is only rearranged by the low-temperature annealing process of a short duration, as has been pointed out by Lin and Wu [8]. This imperfect reverse transformation leaves a residual inelastic strain upon total unloading.

Fig. 3 represents the variation with annealing temperature of the transition stress for the stress-induced martensite formation and the yield stress of the resulting martensite. The transition stress shows an almost constant level at annealing temperatures below 573 K and then decreases with an increase in the annealing temperature until reaching 773 K. After that, it is almost constant while the annealing temperature is increased. The tran-

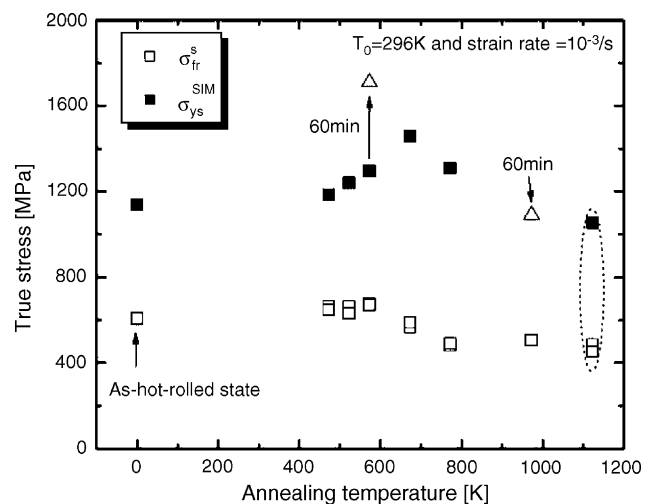


Fig. 3. Variation of the transition stress for the stress-induced martensite formation and the yield stress of the resulting martensite for various annealing temperatures and 10 min duration. The 1123 K case (marked by dotted circle) is annealed for 15 min, and triangle symbols are for those annealed for 60 min.

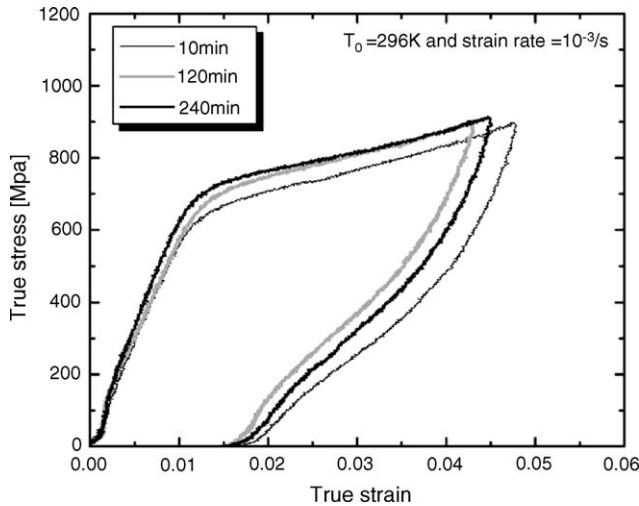


Fig. 4. Variation of the stress–strain curves for a Ni–Ti–Cr alloy annealed at 473 K for the indicated durations.

sition stress decreases from 600 MPa at the as-hot-rolled state to about 470 MPa at an annealing temperature of 1123 K. However, the yield stress of the resulting martensite increases gradually with the increasing annealing temperature, reaching a maximum value of about 1450 MPa at 673 K, due to the precipitation hardening of the alloy. After reaching the maximum level, the yield stress decreases continuously with a further increase in the annealing temperature, because of the recrystallization. Prolonging the annealing at 573 K from 10 to 60 min shows that the yield stress of the resulting martensite increases substantially, from 1300 to 1700 MPa (open triangles marked by an arrow), as the resistance to the dislocation motion is increased due to precipitation hardening [22]. At an annealing temperature of 973 K, there is little change in the yield stress of the resulting martensite (open triangles).

3.2. Annealing duration effect

To maximize the transition stress for the stress-induced martensite formation, samples are heat treated at several selected temperatures for various time periods, as summarized in Table 1. Fig. 4 shows the superelastic behavior of the alloy annealed at 473 K for 10, 120, and 240 min, respectively. The stress–strain curves are almost the same, but the transition stress for the stress-induced martensite formation increases slightly with the increase in the annealing duration. In addition, the annealed alloy shows a permanent residual strain, indicating an imperfect superelasticity. Fig. 5 exhibits the superelastic behavior of the alloy annealed at 573 K for the indicated durations. As the annealing duration increases, the forward and the reverse transformation stresses increase, whereas the residual strain decreases. In particular, a reverse transformation plateau emerges as the annealing duration increases. However, the superelastic response of the samples that were annealed at 773 K is quite different from that of the samples, which had been annealed at 573 K.

Fig. 6 displays the superelastic behavior of samples that were annealed at 773 K for 10, 30, and 60 min, respectively. Unlike those that were annealed at temperatures below 573 K,

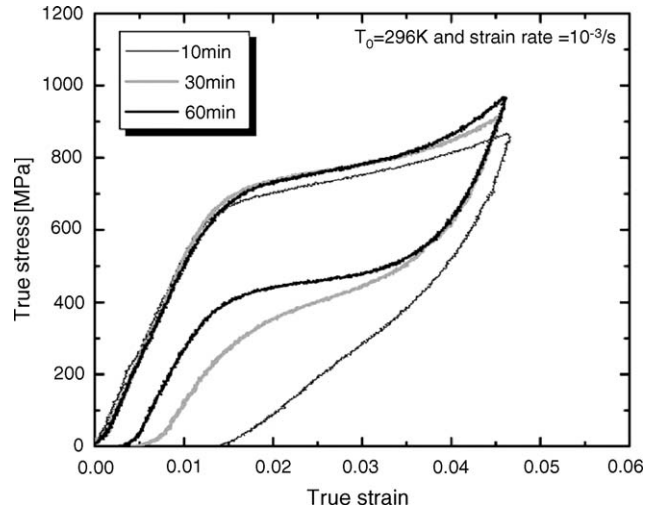


Fig. 5. Variation of the stress–strain curves for a Ni–Ti–Cr alloy annealed at 573 K for the indicated durations.

at a 773 K annealing temperature the transition stresses for the stress-induced martensite formation and the reverse transformation decrease with the increasing annealing duration. The measured residual strain of all specimens, however, is negligibly small.

The variation of the transition stress for the stress-induced martensite formation with the annealing temperature and annealing duration is summarized in Fig. 7. As shown in Fig. 7, the transition stress for the stress-induced martensite formation decreases with an increase in the annealing temperature from 543 to 773 K. After that, it reaches an almost constant level; but a slight increase is seen for annealing at 973 K. The highest transition stress is obtained at an annealing temperature of approximately 573 K. Of particular interest is that, the transition stress for the stress-induced martensite formation for the alloy annealed at temperatures below 573 K, increases with the increasing annealing duration (solid arrow), whereas at annealing temperatures above 573 K, the transition stress decreases

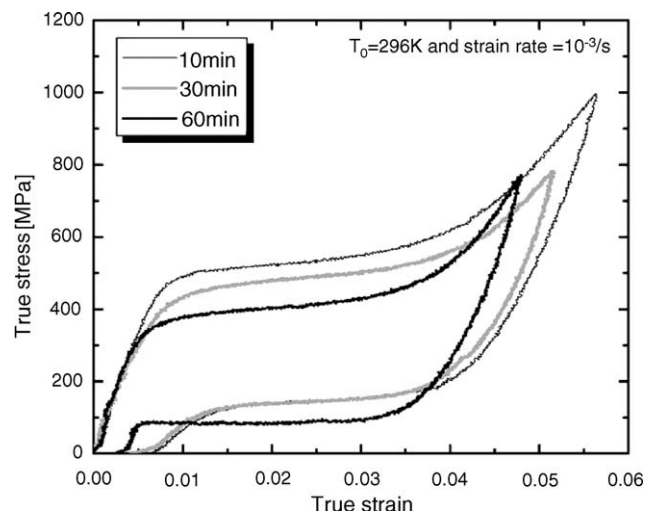


Fig. 6. Variation of the stress–strain curves for a Ni–Ti–Cr alloy annealed at 773 K for the indicated durations.

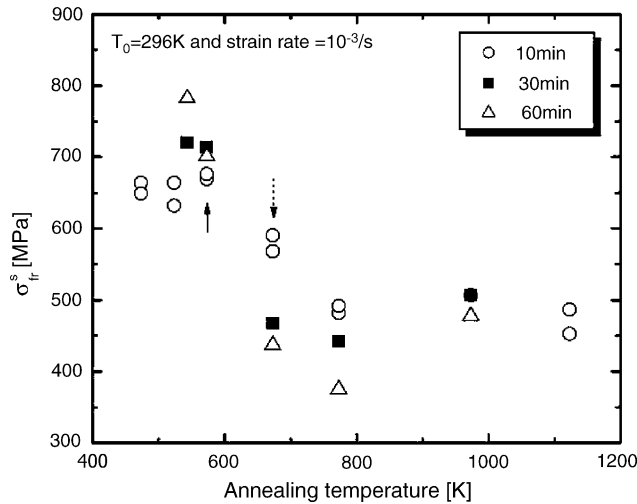


Fig. 7. Variation of the transition stress for the stress-induced martensite formation as a function of annealing temperature for the indicated durations.

(dotted arrow). These variations are related to the precipitation behavior of the Ni–Ti–Cr alloy.

Fig. 8 exhibits the precipitates of undeformed samples that were annealed at 573, 673, and 773 K for 60 min, respectively. According to the study of the precipitation behavior in Ni–Ti

alloy [23,24], the Ti_3Ni_4 precipitates strongly affect the mechanical property of Ni-rich Ni–Ti alloys. Therefore, the complex precipitate, $Ti_3(Ni, Cr)_4$, some of whose Ni is replaced by Cr, is expected to be formed in the Ni–Ti–Cr alloy, with the precipitate size varying appreciably with the annealing temperature and duration. The precipitates are nanometer-sized clusters in Fig. 8(a) and micrometer-sized platelets in Fig. 8(c). The nanometer-sized clusters produce a maximum transition stress for the stress-induced martensite formation, as shown in Fig. 7. Furthermore, it is also observed that the transition stress decreases with the increasing precipitate size. This is due to the variation of the material's stability and the resistance to dislocation motion with the precipitate size. According to the study of Ti–50.9 at.% Ni by Gall et al. [21,25] the transformation temperature, M_s , increases with the increasing precipitate size up to 100 nm precipitate, and then it decreases as the precipitate size increases.

DSC results of a Ni–Ti–Cr alloy that was annealed at different temperatures for 60 min, are shown in Fig. 9. The curve obtained from a sample which was annealed at 973 K, exhibits a single transformation sequence (austenite to martensite and reverse) of this alloy, $A \leftrightarrow M$, as shown in Fig. 9(a). The obtained M_s and A_f temperatures are 257 and 280 K, respectively. As is seen in Fig. 9(b), as the annealing temperature decreases from

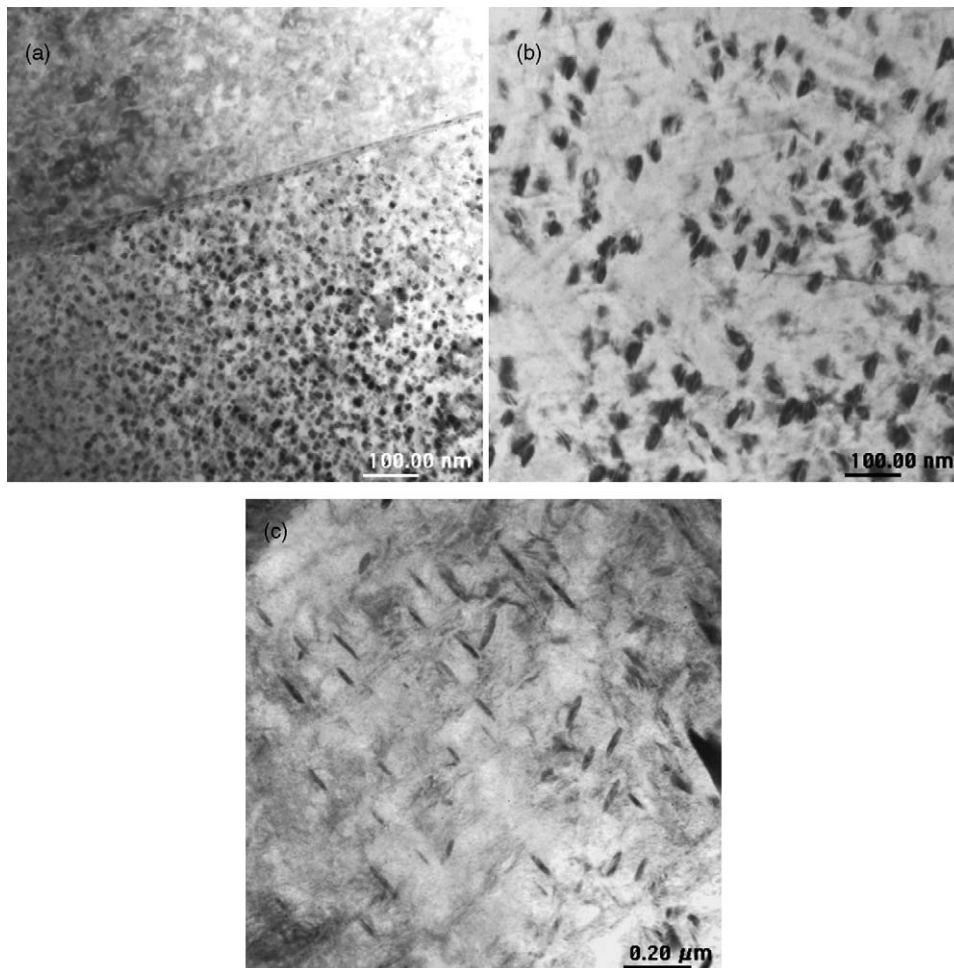
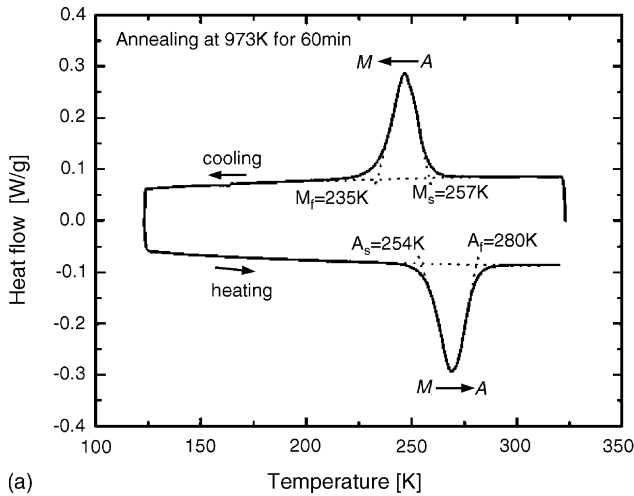
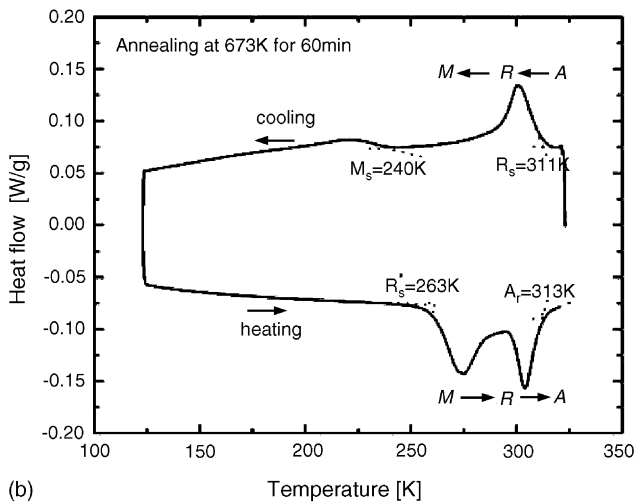


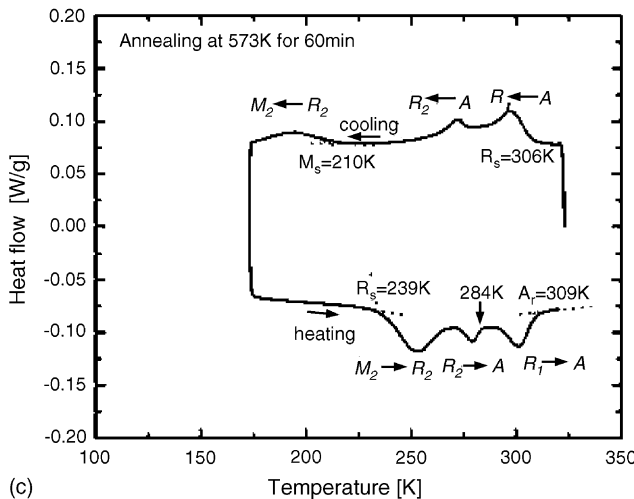
Fig. 8. TEM micrographs of a Ni–Ti–Cr alloy annealed for 60 min at: (a) 573 K, (b) 673 K, and (c) 773 K.



(a)



(b)



(c)

Fig. 9. Transformation curves of Ni–Ti–Cr alloy annealed at: (a) 973 K, (b) 673 K, and (c) 573 K.

973 to 673 K, a single forward transformation, $A \rightarrow M$, evolves into a two-step transformation, $A \rightarrow R \rightarrow M$ (austenite to rhomboidal to martensite). Moreover, the reverse transformation upon heating, $M \rightarrow A$, also shows a two-step transformation behavior, $M \rightarrow R \rightarrow A$. As the annealing temperature further decreases to

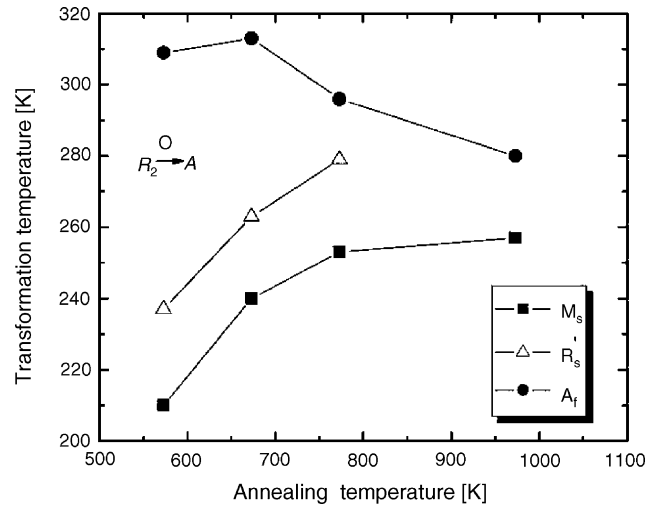


Fig. 10. Transformation temperatures of Ni–Ti–Cr alloy annealed at different temperatures for 60 min.

573 K, a two-step transformation behavior evolves into a three-step transformation, as shown in Fig. 9(c). These results are different from the results of Uchil et al. [20] who suggest that the $A \leftrightarrow R$ transformation in Ni–Ti–Cr alloy is only observed at annealing temperatures below 673 K. A similar three-step transformation in Ni–Ti alloys has also been observed when annealing the material at low temperatures. According to Kim et al. [26], these phase transformation steps in 50.9 at.% Ni–Ti alloy can be $A \rightarrow R_1$, $A \rightarrow R_2$, and $R_2 \rightarrow M_2$, during the cooling process, and $M_2 \rightarrow R_2$, $R_2 \rightarrow A$, and $R_1 \rightarrow A$, during the heating process. Here, R_1 denotes the R -phase formed around the precipitates, R_2 denotes the R -phase formed in the regions away from precipitates, and M_2 denotes the martensite formed from the R_2 -phase. This multiple-step transformation is explained in terms of the inhomogeneity of the composition [11], internal stress field [27], and both composition and internal stress [12], associated with the precipitates, Ti_3Ni_4 . The transformation and the corresponding annealing temperatures for this alloy are summarized in Fig. 10. The M_s temperature increases with the increasing annealing temperature, indicating that the relative stability of the austenite, i.e. the temperature difference between M_s and the initial sample temperature, 296 K, decreases. A similar result is also obtained by Gall et al. [21,25]. Moreover, this result agrees well with the mechanical properties shown in Fig. 7.

In addition, the yield stress of the resulting martensite in Fig. 3 depends on the precipitate size. Small precipitates lead to a higher yield stress. These trends are the same as those reported by Treppmann et al. [28] and Ishida and Miyazaki [29], who point out that the critical resolved shear stress for the dislocation motion reaches a maximum level at approximately 10 nm precipitates. After this, the stress decreases towards its saturation value, as the precipitate size increases further, up to about 500 nm. In the present work, we have sought to determine an optimum annealing condition that results in an excellent transition and yield stresses for the stress-induced martensite, without a residual strain. We have concluded that this can be attained by annealing at a 573 K for 60 min.

3.3. Initial temperature effect

To study the effect of initial temperature on the superelastic response of our Ni–Ti–Cr alloy, compression tests are performed at a strain rate of $10^{-3}/s$ over the temperature range of 230–400 K. Before testing, a Ni–Ti–Cr alloy is annealed at 573 K for 60 min. According to the DSC result in Fig. 9(c), the specimen has a fully austenite state at temperatures above 306 K, but upon cooling, it has a mixture of rhomboidal and austenite phases in the 306–277 K temperature range. A single martensite phase exists at temperatures below 239 K, and, upon heating, a mixture of rhomboidal and austenite phases from 239 to 309 K, and a full austenite phase at temperatures above 309 K. Fig. 11 shows the effect of initial temperature on

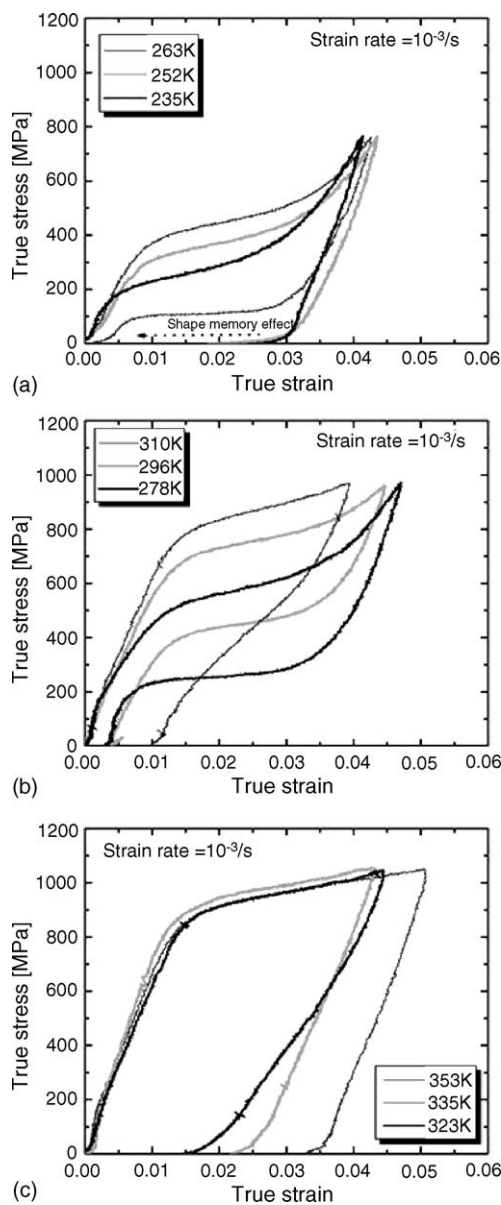


Fig. 11. Stress–strain curves for a Ni–Ti–Cr alloy annealed at 573 K, deformed at the indicated initial sample temperatures and a $10^{-3}/s$ strain rate: (a) initial temperature below 263 K, (b) initial temperature from 263 to 323 K and (c) initial temperature above 323 K.

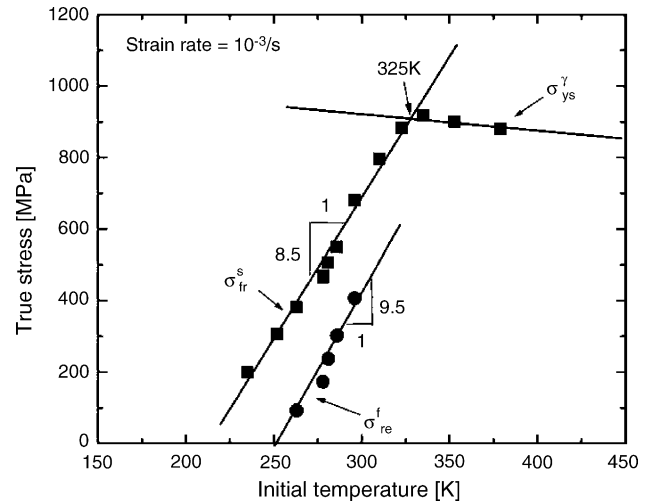


Fig. 12. Variation of the transition stress as a function of initial temperature.

the stress–strain response of the annealed alloy. As is seen, the stress–strain curves strongly depend on the initial temperature. The curves in Fig. 11(a), obtained at initial temperatures below 263 K, show large residual strains, which however are not permanent. They are recovered at a temperature of 296 K, showing the shape-memory effect. At initial temperatures above 263 K, the stress–strain curves display a superelastic effect, i.e. a hysteresis loop, until the sample temperature reaches 310 K, after which, the residual strain increases with the increasing sample temperature; see Fig. 11(b) and (c). An interesting point is the reverse transformation behavior in the superelastic temperature range. The occurrence of the reverse transformation at temperatures above 323 K is unclear even though the unloading curve shows a small amount of recovered strain. The unloading curve obtained for 310 K, has an inflection point, indicating the reverse transformation of the stress-induced martensite to the austenite. At an initial temperature below 296 K, the unloading stress–strain curve clearly shows a plateau regime that corresponds to the reverse transformation.

Fig. 12 exhibits the temperature dependence of the transition stresses for the stress-induced martensite and the reverse transformation, and the yield stress of the austenite, at a strain rate of $10^{-3}/s$. The transition stress for the stress-induced martensite formation increases with the increasing initial temperature. This is in line with the Clausius–Clapeyron equation that gives a relation between the initial temperature and the critical stress for the stress-induced martensite formation [30]. The yield stress of the austenite, however, decreases with the increase in the temperature. The $d\sigma_{fr}^s/dT$ at a strain rate of $10^{-3}/s$ is approximately 8.5 MPa/K. This value is greater than 7.3 MPa/K in polycrystalline Ni–Ti alloys that which is obtained under quasi-static states [31–33]. The M_d temperature, i.e. the maximum temperature for the stress-induced martensite formation, is determined by the intersection of the slope of the transition stress and the dislocation-induced slip stress versus temperature lines. The M_d temperature at a $10^{-3}/s$ strain rate is about 325 K, in agreement with the residual strain behavior. The finishing stress for the reverse transformation, σ_{re}^f , is measured and plotted in

Fig. 12. The Clausius-Clapeyron slope for the reverse transformation is about 9.5 MPa/K, which is greater than that of the transition stress for the stress-induced martensite formation, i.e. 8.5 MPa/K.

4. Conclusions

Compressive tests are performed on cylindrical samples to investigate the effect of the annealing conditions and the initial temperature on the mechanical response of a Ni–Ti–Cr shape-memory alloy, deformed at a 10^{-3} /s strain rate, using an Instron hydraulic testing machine. Several noteworthy conclusions are as follows:

- (1) For a duration time of 10 min, the transition stress for the stress-induced martensite formation remains almost constant for annealing temperatures below 573 K. After that, it decreases with an increase in the annealing temperature, and finally remains almost constant. The yield stress of the resulting martensite, however, attains a maximum value when the annealing temperature reaches about 673 K.
- (2) The transition stress for the stress-induced martensite formation increases with the increasing annealing duration at annealing temperatures below 573 K, whereas it decreases for annealing temperatures above 573 K. A transition stress in the reverse transformation is clearly retained while the annealing duration is increased, except for the annealing temperature of 473 K.
- (3) The variation of the transition stress with the annealing duration and temperature is closely related to the size of the precipitates. The smallest precipitates that occur in annealing at 573 K for 60 min, produce the maximum stress. This stress decreases as the size of the precipitates increases.
- (4) The phase transformation step in the cooling and heating processes depends on the annealing temperature. A single step transformation at a 973 K annealing temperature changes into a multiple-step transformation with decreasing annealing temperature. A three-step transformation is clearly observed upon heating and cooling, for a specimen that was annealed at 573 K.
- (5) The transition stress of the stress-induced martensite increases at a 8.5 MPa/K rate with an increase in initial temperature. The M_d is approximately 325 K at a 10^{-3} /s strain rate.
- (6) Considering all annealing conditions, the optimum annealing condition producing the highest transition and yield stresses without a residual strain, is determined to be 573 K for 60 min. The attained transition stress is about 700 MPa and the yield stress of the resulting martensite is about 1700 MPa.

Acknowledgements

This work was supported by ONR (MURI) grant N000140210666 to the University of California, San Diego. The authors wish to express their appreciation to Mr. G.-Y Ryu at RIST, Korea, for helping with the TEM microstructural observations.

References

- [1] S. Miyazaki, K. Otsuka, *ISIJ Int.* 29 (1989) 353–377.
- [2] K. Otsuka, C.M. Wayman, in: K. Otsuka, C.M. Wayman (Eds.), *Shape Memory Materials*, Cambridge University Press, Cambridge, 1998, pp. 1–48.
- [3] J. Van Humbeeck, *Mater. Sci. Eng. A* 237–275 (1999) 134–148.
- [4] J. Van Humbeeck, *Adv. Eng. Mater.* 3 (2001) 143–156.
- [5] S. Saadat, J. Salichs, M. Noori, H. Davood, I. Bar-On, Y. Suzuki, A. Masuda, *Smart Mater. Struct.* 11 (2002) 218–229.
- [6] D. Tirelli, S. Mascelloni, *J. Phys. IV* 10 (2000) 665–670.
- [7] Y. Liu, P.G. McCormick, *ISIJ Int.* 29 (1989) 417–422.
- [8] H.C. Lin, S.K. Wu, *Acta Mater.* 42 (1994) 1623–1630.
- [9] E. Hornbogen, *J. Mater. Sci.* 34 (1999) 599–606.
- [10] J. Zhang, X. Ren, K. Otsuka, M. Asai, *Scripta Mater.* 41 (1999) 1109–1113.
- [11] J.K. Allafi, X. Ren, G. Eggeler, *Acta Mater.* 50 (2002) 793–803.
- [12] D. Chrobak, D. Stroz, H. Morawiec, *Scripta Mater.* 48 (2003) 571–576.
- [13] X. Huang, Y. Liu, *Scripta Mater.* 45 (2001) 153–160.
- [14] S. Nemat-Nasser, W.-G. Guo, *Mech. Mater.* 38 (2006) 463–474.
- [15] K.N. Melton, O. Mercier, *Metall. Trans.* 9A (1978) 1487–1488.
- [16] T.H. Nam, T. Saburi, K. Shimizu, *Mater. Trans. JIM* 31 (1990) 959–967.
- [17] M. Piao, S. Miyazaki, K. Otsuka, *Mater. Trans. JIM* 33 (1992) 346–353.
- [18] S.F. Hsieh, S.K. Wu, *J. Mater. Sci.* 34 (1999) 1659–1665.
- [19] M. Nishida, C.M. Wayman, T. Honea, *Metallography* 19 (1986) 99–113.
- [20] J. Uchil, K.K. Ganesh, K.K. Mahesh, *J. Alloys Compd.* 325 (2001) 210–214.
- [21] K. Gall, K. Juntunen, H.J. Maier, H. Sehitoglu, Y.I. Chumlyakov, *Acta Mater.* 49 (2001) 3205–3217.
- [22] H. Sehitoglu, I. Karaman, R. Anderson, X. Zhang, K. Gall, H.J. Maier, Y. Chumlyakov, *Acta Mater.* 4 (2000) 3311–3326.
- [23] T. Tadaki, Y. Nakada, K. Shimizu, K. Otsuka, *Mater. Trans. JIM* 27 (1986) 731–740.
- [24] K. Gall, H. Sehitoglu, Y.I. Chumlyakov, I.V. Kireeva, H.J. Maier, *J. Eng. Mater. Technol.* 121 (1999) 19–27.
- [25] K. Gall, H.J. Maier, *Acta Mater.* 50 (2002) 4643–4657.
- [26] J.I. Kim, Y. Liu, S. Miyazaki, *Acta Mater.* 52 (2004) 487–499.
- [27] L. Bataillard, J.-E. Bidaux, R. Gotthardt, *Phil. Mag.* 78 (1998) 327–344.
- [28] D. Treppmann, E. Hornbogen, D. Wurzel, *J. Phys. V C8* (1995) 569–574.
- [29] A. Ishida, S. Miyazaki, *J. Eng. Mater. Technol.* 121 (1999) 2–8.
- [30] P. Wollants, J.R. Roos, L. Delaey, *Prog. Mater. Sci.* 37 (1993) 227–288.
- [31] K. Jacobus, H. Sehitoglu, M. Balzer, *Metall. Trans.* 27A (1996) 3066–3073.
- [32] Y. Liu, S.P. Galvin, *Acta Mater.* 45 (1997) 4431–4439.
- [33] K. Gall, H. Sehitoglu, Y.I. Chumlyakov, I.V. Kireeva, H.J. Maier, *J. Eng. Mater. Technol.* 121 (1999) 28–37.